

01 Nov 2005

Solids Flow Mapping in a High Pressure Slurry Bubble Column

Novica Rados

Ashfaq Shaikh

Muthanna H. Al-Dahhan

Missouri University of Science and Technology, aldahhanm@mst.edu

Follow this and additional works at: https://scholarsmine.mst.edu/che_bioeng_facwork



Part of the [Biochemical and Biomolecular Engineering Commons](#)

Recommended Citation

N. Rados et al., "Solids Flow Mapping in a High Pressure Slurry Bubble Column," *Chemical Engineering Science*, vol. 60, no. 22, pp. 6067 - 6072, Elsevier, Nov 2005.

The definitive version is available at <https://doi.org/10.1016/j.ces.2005.04.087>

This Article - Conference proceedings is brought to you for free and open access by Scholars' Mine. It has been accepted for inclusion in Chemical and Biochemical Engineering Faculty Research & Creative Works by an authorized administrator of Scholars' Mine. This work is protected by U. S. Copyright Law. Unauthorized use including reproduction for redistribution requires the permission of the copyright holder. For more information, please contact scholarsmine@mst.edu.

Solids flow mapping in a high pressure slurry bubble column

Novica Rados¹, Ashfaq Shaikh, Muthanna H. Al-Dahhan*

Chemical Reaction Engineering Laboratory, Department of Chemical Engineering, Washington University in St. Louis, Campus Box 1198, One Brookings Dr., St. Louis, MO 63130-3899, USA

Received 1 February 2005; received in revised form 19 April 2005; accepted 20 April 2005
Available online 15 July 2005

Abstract

Successful design and scale-up of Slurry Bubble Column Reactors (SBCRs) require proper understanding of how operating conditions affect their flow behavior. Presently, there is little information on the flow dynamics of solids (e.g., distribution of velocities and turbulent parameters) in slurry systems that are operated at industrially relevant conditions of high pressure, high superficial gas velocities, and high solids loading.

Computer Automated Radio Particle Tracking (CARPT) is widely recognized as one of a few techniques that can be reliably used even in highly turbulent and opaque slurry flows. This work utilizes an improved CARPT technique to investigate the effect of reactor pressure (0.1–1 MPa) and superficial gas velocity (0.08–0.45 m/s) on solids phase velocity and shear stress in a pilot scale 0.16 m diameter stainless steel column using an air–water–glass beads (150 μm) system. The solids axial velocity and shear stress were found to increase noticeably with pressure and superficial gas velocity in the churn turbulent flow regime.

© 2005 Elsevier Ltd. All rights reserved.

Keywords: Slurry bubble column; CARPT; Solids velocity; Shear stress

1. Introduction

Slurry bubble column reactors (SBCRs) are cylindrical vessels in which gas is sparged into a suspension of liquid and fine solids (typically catalyst). The size of the solids (catalyst) ranges from 5 to 150 μm , and the solids loading is up to 50% by volume (Krishna et al., 1997). The gas phase contains one or more reactants, while the liquid phase usually contains product and/or reactant (or sometimes is inert). These reactors are of considerable interest in industrial processes such as oxidation, hydrogenation of heavy oils, Fischer-Tropsch synthesis, liquid phase methanol synthesis, chlorination, alkylation, wastewater treatment, and various biochemical processes (Deckwer and Alper, 1980; Dry, 1982; Fan, 1989). In SBCR, two types of flow regimes exist: a homogeneous or bubbly flow regime (at low

superficial gas velocity, where bubbles rise without much interaction) and a heterogeneous or churn-turbulent flow regime (at high superficial gas velocity, where bubbles churn through the slurry experiencing a high rate of breakage and coalescence). SBCRs are simple in construction, yet the mixing characteristics and fluid dynamics of these vessels are complex due to complex interaction among phases. The proper design and scale-up of SBCRs require a thorough understanding of how various design parameters (reactor geometry, internals, sparger design, etc.) and operating variables (reactor pressure and temperature, gas and liquid flow rates, catalyst size and loading, liquid phase properties, etc.) affect the system fluid dynamics.

Most of the reported hydrodynamic studies in bubble (two phases) and slurry bubble (three phases) columns have been conducted at low superficial gas velocities and atmospheric pressure. Moreover, due to lack of proper measurement techniques, the available studies at high superficial gas velocities and high operating pressures are limited to overall gas holdup, overall liquid-side mass transfer coefficient, pressure drop, and tracer studies.

* Corresponding author. Tel.: +1 314 935 7187; fax: +1 314 935 4832.

E-mail address: muthanna@seas.wustl.edu (M.H. Al-Dahhan).

¹ Current address: ExxonMobil Research and Engineering, 3225 Gal-lows Rd., Rm. 8A 1730, Fairfax, VA 22037-0001, USA.

The studies at low superficial gas velocities and atmospheric pressure show qualitative similarity between liquid phase velocity in bubble columns (gas–liquid, G–L) and solids phase velocity in slurry bubble columns (gas–liquid–solid, G–L–S) (Degaleesan, 1997; Sannaes, 1997). Studies of bubble column hydrodynamics indicate the presence of a single recirculation cell in the time-averaged sense, with liquid flowing up in the center and flowing downwards close to the wall in the fully developed region (Degaleesan, 1997). In the churn-turbulent flow regime, the gas is non-uniformly distributed across the column cross-section, with highest gas holdup in the center region of the column and lowest gas holdup in the wall region. The non-uniform distribution of gas holdup across the cross-section together with the gas dynamics (bubble size and rise velocity, interfacial area, local gas holdup distributions) drives the liquid/slurry recirculation. Hence, the axial velocity radial profile shows the maximum value in the center of column and decreases monotonically towards the column wall achieving negative velocity in the region near the wall to satisfy the mass balance. The radial position where the axial velocity equals zero, called the inversion point, is typically located around dimensionless radius of 0.6–0.7 (Degaleesan, 1997; Sannaes, 1997). The axial component of the velocity has been found to be the highest in magnitude, while the radial component is relatively negligible. Earlier studies by Degaleesan (1997) and Sannaes (1997) showed that superficial gas velocity affects the axial liquid/solid velocity profile. It increases with an increase in superficial gas velocity, while the effect of column diameter and solids loading (at low range of magnitude) on the axial velocity profiles is relatively less pronounced. For most industrial applications, bubble and slurry bubble columns are operated at high superficial gas velocities and high operating pressure. As mentioned earlier, due to the limitations of the available measurement techniques, the effect of high superficial gas velocity and operating pressure on the velocity profiles in slurry bubble columns has not been studied.

Computer Automated Radioactive Particle Tracking (CARPT), which is used extensively on various multiphase flow systems at the Chemical Reaction Engineering Laboratory (CREL, 1993), Washington University, is a non-invasive technique for tracking a single radioactive tracer particle. The tracer particle follows the motion of the tracked phase (for liquid a neutrally buoyant particle, and for solids, a particle of the same size and density). Its position is determined by detecting the intensity distribution of emitted γ -rays, using an array of NaI scintillation detectors. The collected radiation intensity data is first used to reconstruct the tracer particle trajectory based on calibration data. The particle trajectory (location in time) is then used to estimate tracer particle occurrence, velocity, Reynolds stress, turbulent kinetic energy, and eddy diffusivity profiles, and many other parameters.

The CARPT technique was originally developed and implemented for atmospheric experimentation (Devanathan,

1991; Degaleesan, 1997). Recently, Rados (2003) has improved the CARPT technique and implemented it on high pressure systems to investigate solids fluid dynamics in a 0.162 m diameter stainless steel slurry bubble column. The column can be operated at pressure up to 1.2 MPa and superficial gas velocity up to 0.60 m/s. The improvements include (1) acquisition of the photo-peak data only, (2) development of an automated calibration device that can be used in high pressure vessels, and (3) establishing a more accurate tracer particle location reconstruction algorithm. The details of accuracy of measurements have been explained elsewhere (Degaleesan, 1997; Rammohan, 2003; Rados, 2003), and therefore will not be repeated here.

In the current work, the improved CARPT technique (Rados, 2003) has been utilized to study the effect of superficial gas velocity and operating pressure on mixing characteristics of slurry bubble column reactors, in particular on solids axial velocity and solids shear stress.

2. Experimental setup

The experiments were carried out in a high pressure stainless steel column with an inner diameter of 0.162 m and a height of 2.5 m. Fig. 1 is a schematic diagram of column used in this study. It is designed to support a maximum operating pressure of 1.2 MPa. Air, as the gas phase, was supplied by two compressors connected in parallel, with a working

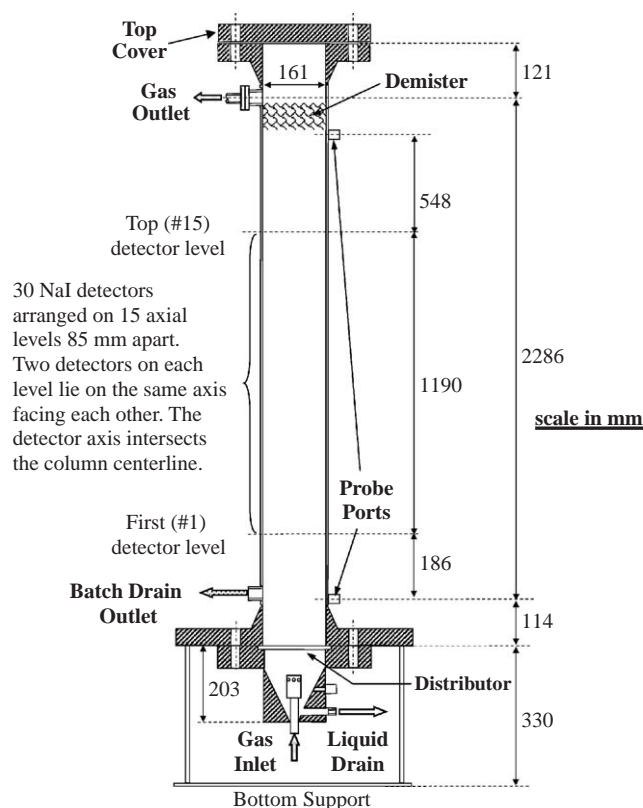


Fig. 1. High pressure slurry bubble column reactor.

pressure of 1.45 MPa and a maximum corresponding flow rate of $8.8 \text{ m}^3/\text{min}$. The compressed atmospheric air was purified by passing it through a dryer and several air filter units. The air flow rate was regulated by a pressure regulator and four rotameters of increasing range connected in parallel. Air exited the column through a demister, passed through a back pressure regulator that controls column operating pressure, and then vented to the ventline. The column design enabled easy removal of the sparger chamber for replacement of the sparger. Water was the liquid phase. Glass beads with an average diameter of $150 \mu\text{m}$ and particle density of 2490 kg/m^3 constituted the solids phase. In all experiments, the dynamic height of slurry was maintained at 1.8 m from the distributor, and the solid loading [ratio of volume of solids to volume of ungasged slurry (solid+liquid)] was kept the same, at 9.1% volume. The experiments were carried out at superficial gas velocities ranging from 0.08 to 0.45 m/s and operating pressures of 0.1–1.0 MPa.

In the present study, 30 NaI scintillation detectors were used. The counts were acquired at the frequency of 50 Hz, and the detected signal was amplified, processed, and recorded (Rados, 2003). The axial span of the detectors covered the middle, fully developed flow portion of the column from 0.30 ($z/D \sim 1.8$) to 1.49 m ($z/D \sim 9.3$) of the height above the sparger (Fig. 1). The radioactive tracer particle was made to resemble as closely as possible the solid phase particles in size and density. Solids tracking in all of the listed experiments was performed using a $\sim 150 \mu\text{m}$ composite scandium, Sc46 tracer particle coated with $\sim 6 \mu\text{m}$ thin Parylene N (a uniform, chemically inert, and mechanically strong coating material). The composite tracer particle density was estimated to be between 2400 and 2550 kg/m^3 , closely resembling solids particle density of 2490 kg/m^3 (Rados, 2003). The activity of the scandium Sc46 tracer particles at the time of the experiments was estimated at about 1.9 MBq ($50 \mu\text{Ci}$).

Provided the observation time period is large enough (in our case, it was 24 hours) and tracer adequately mimics the solids in the system, the information yielded in the ‘time averaged’ sense by one tracer particle is the same as conveyed in ‘ensemble averaged’ sense.

The combination of calibration and actual experimental run provides the sequence of instantaneous position data that yields the position of particle at successive sampling instants. Time differentiation of successive particle positions gives instantaneous Lagrangian velocities of the particle, i.e., velocities as a function of time and position. From the Lagrangian particle velocities, ‘ensemble averaging’ is performed to calculate the averaged velocities. In a sense, Lagrangian velocities are converted to time-averaged Eulerian flow field with an assumption of ‘ergodicity’.

3. Results

Figs. 2 and 3 show the solids flow pattern and time and azimuthally averaged solids velocity profiles in an

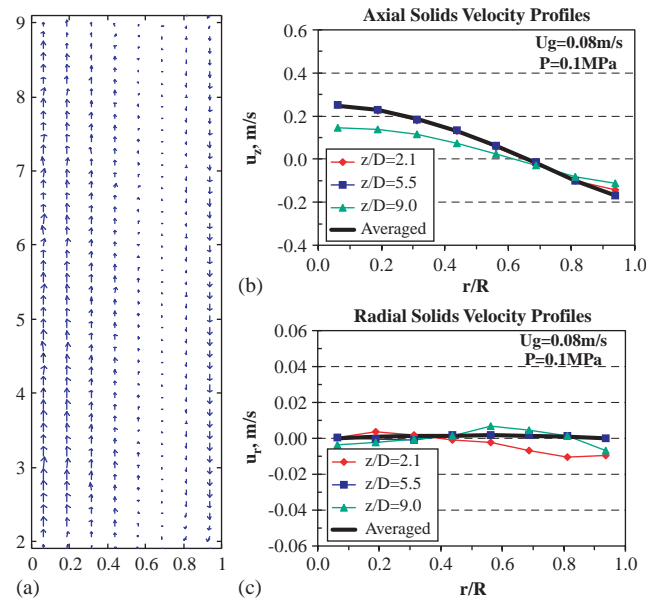


Fig. 2. Time- and azimuthally-averaged solids velocity radial profiles in an air–water-($150 \mu\text{m}$) glass beads system operated at $U_G = 0.08 \text{ m/s}$, pressure of 0.1 MPa, and solids loading = 9.1% volume. (a) $u_z - u_r$ vector map, (b) axial velocity component and (c) radial velocity component.

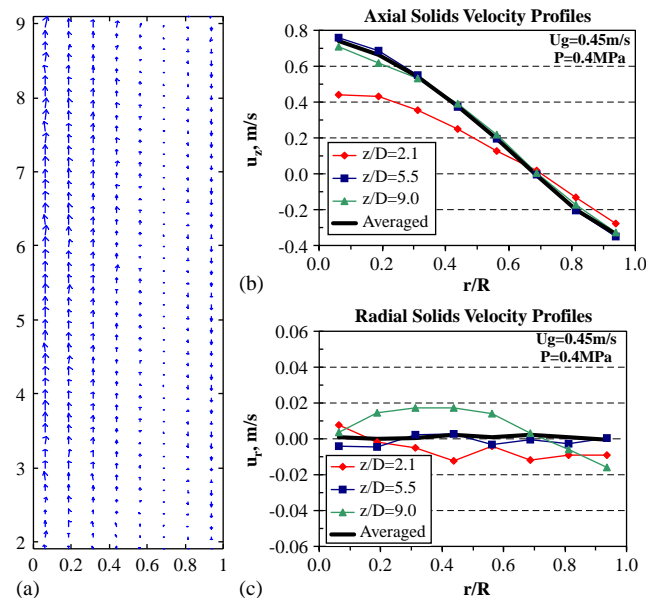


Fig. 3. Time- and azimuthally-averaged solids velocity radial profiles in an air–water-($150 \mu\text{m}$) glass beads system operated at $U_G = 0.45 \text{ m/s}$, pressure of 0.4 MPa, and solids loading = 9.1% volume. (a) $u_z - u_r$ vector map, (b) axial velocity component and (c) radial velocity component.

air–water–glass beads ($150 \mu\text{m}$) system with solids loading of 9.1% volume at (1) $U_G = 0.08 \text{ m/s}$ and $P = 0.1 \text{ MPa}$ and (2) $U_G = 0.45 \text{ m/s}$ and $P = 0.4 \text{ MPa}$, respectively. A typical single cell slurry flow recirculation pattern is observed in vector plots (Figs. 2a and 3a). This flow pattern is characterized with the slurry up-flow (positive axial velocity) in the central region of the column and the

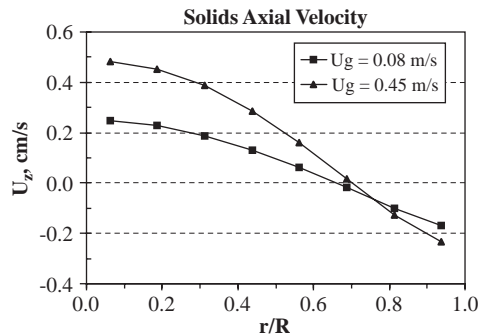


Fig. 4. Effect of superficial gas velocity on the time-, azimuthally-, and axially-averaged solids axial velocity radial profiles using air–water–glass beads ($150\ \mu\text{m}$) system at solids loading of 9.1% volume in 0.16 m diameter slurry bubble column at atmospheric pressure.

down-flow (negative axial velocity) in the annular region, near the column wall. The fully developed flow extends axially between approximately $2D$ (0.32 m) and $H_D - D$ (1.63 m) ($2D < z < H_D - D$), where H_D is the dynamic height and z is the height from the distributor. The radial velocity component is small in the fully developed flow region ($U_r < 0.02\ \text{m/s}$). However, its magnitude increases in the entry ($z < D$) and the disengagement ($z > H_D - D$) regions of the column, particularly for high superficial gas velocity ($U_G = 0.45\ \text{m/s}$).

The axial and radial velocity components across the radius of the column are presented at three axial locations, i.e., $z = 2.1D$, $5.5D$, and $9D$. The averaged velocity in Figs. 2 and 3 is the one averaged axially from $z = 2D$ to $H_D - D$, which represents the fully developed flow region. One can see that the solids axial velocities at $z/D = 2.1$ and 5.5 are similar to the averaged velocity at $U_G = 0.08\ \text{m/s}$ (Fig. 2). At $z/D = 5.5$ and 9.0 the velocities are similar to the averaged velocity at $U_G = 0.45\ \text{m/s}$ (Fig. 3). At $z/D = 9.0$ ($U_G = 0.08\ \text{m/s}$, Fig. 2) and $z/D = 2.1$ ($U_G = 0.45\ \text{m/s}$, Fig. 3), the axial velocity is lower and radial velocity is slightly higher than the average of these velocity components. This finding confirms that these z/D at the indicated conditions are at the edges of the fully developed flow region.

3.1. Effect of superficial gas velocity

Fig. 4 shows the effect of superficial gas velocity (SGV) on the radial profile of time-, axially-, and azimuthally-averaged solids axial velocity in an air–water–glass beads ($150\ \mu\text{m}$) system with solids loading of 9.1% volume at atmospheric pressure. An increase in superficial gas velocity increases the solids axial velocity component. Higher superficial gas velocity results in higher positive as well as negative solids axial velocities, and thus in larger circulation. The increase in axial solids velocity is the result of the increase in the gas holdup and the steepness of the gas holdup profile at $0.45\ \text{m/s}$ compared to $0.08\ \text{m/s}$ (Rados et al., 2005).

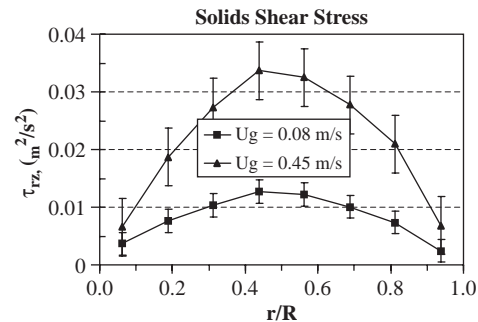


Fig. 5. Effect of SGV on solids shear stress radial profiles using air–water–glass beads ($150\ \mu\text{m}$) system at solids loading of 9.1% volume in 0.16 m diameter slurry bubble column at atmospheric pressure.

Fig. 5 shows the effect of superficial gas velocity on the radial profile of the time-, axially-, and azimuthally-averaged solids shear stress. Solids shear stress is directly proportional to the radial gradient of axial velocity (Ueyama and Miyauchi, 1979) based on the Boussinesq hypothesis, which is frequently used as closure for one-dimensional liquid recirculation model (Kumar, 1994). The use of the Boussinesq hypothesis to explain shear stress behavior can be questionable, but not many options are available. An increase in superficial gas velocity increases the solids axial velocity, and also its gradient that results in higher shear stress at higher superficial gas velocities. The shear stress is close to zero in the center and near the column wall. The maximum in the shear stress value is related to the inversion point in axial velocity, as it exhibits the highest velocity gradient in this region. The error bars in solids shear stress figures represent one standard deviation from averaged shear stress along the axial coordinate at every radial location.

3.2. Effect of operating pressure

Fig. 6 shows the effect of operating pressure on the radial profile of time-, axially-, and azimuthally-averaged solids axial velocity in an air–water–glass beads ($150\ \mu\text{m}$) system with solids loading of 9.1% volume at superficial gas velocity of 0.08 and 0.45 m/s. Previous studies (Kemoun et al., 2001; Rados et al., 2005) have shown that an increase in operating pressure at the same superficial gas velocity results in an increased magnitude of the gas holdup profile. Because the gas holdup profile drives the liquid circulation in bubble/slurry columns, higher pressure results in higher solids axial velocity due to increased gas holdup. Xue (2004) developed a four-point optical probe for bubble velocity, bubble size, and interfacial area measurement in bubble columns. He conducted experiments in air–water system at atmospheric and high pressure (0.4 and 1 MPa). He concluded that with an increase in pressure the mean velocity of bubbles moving upwards increases and of those moving downwards decreases in the column center, while the downward movement of bubbles is enhanced in the wall zone. His

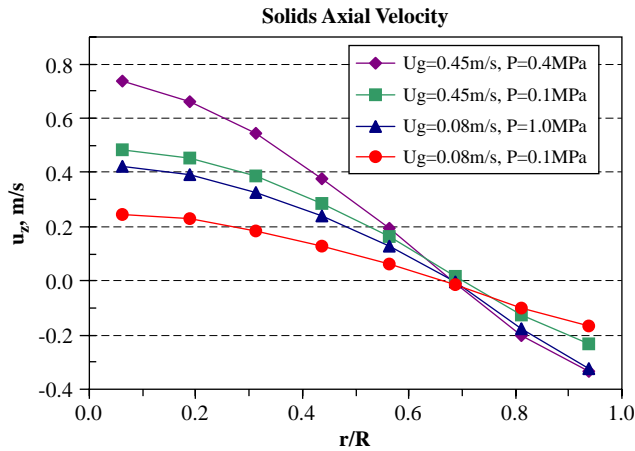


Fig. 6. Effect of operating pressure on the solids axial velocity radial profiles using air–water–glass beads ($150\ \mu\text{m}$) system at solids loading of 9.1% volume in 0.16 m diameter slurry bubble column.

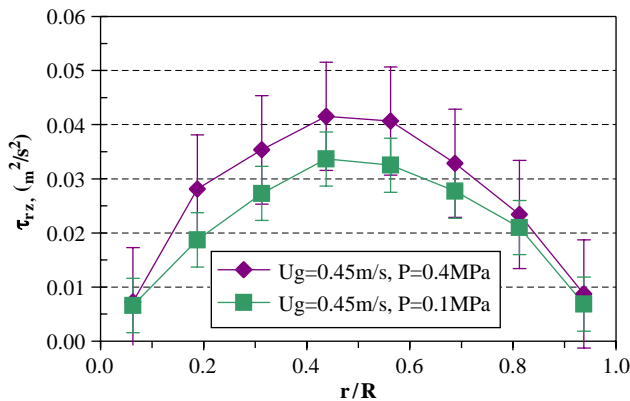


Fig. 7. Effect of operating pressure on the solids shear stress radial profiles using air–water–glass beads ($150\ \mu\text{m}$) system at solids loading of 9.1% volume in 0.16 m diameter slurry bubble column.

study showed that in the center the population of small bubbles considerably increases with pressure that contributes to an increase in gas holdup. This results into increased gradient of buoyancy between the column center and the wall region resulting in enhanced liquid/slurry circulation.

Fig. 7 shows the effect of operating pressure on radial profile of solids shear stress at 0.45 m/s. Solids shear stress at high pressures shows similar trend as the one at atmospheric pressure, with value close to zero in the center and near the wall and maximum around the region of the inversion point. High pressure results in higher axial velocity and its gradient. Because the shear stress is proportional to the velocity gradient, it leads to higher shear stresses at increased pressure. The higher pressure reduces the steepness of the gas holdup profile due to existence of smaller bubbles, the effect that may result in lower velocity fluctuations. However, because of the higher mean axial velocity gradient, the net result is higher shear stress.

In this study, the only deviation from this trend is observed in a system that is operated at $U_G = 0.08\ \text{m/s}$. The maximum value of shear stress at $P = 0.1\ \text{MPa}$ was found to be higher than the one at $P = 1.0\ \text{MPa}$. Also, in the center, shear stress at 1 MPa was lower while near the wall, it was higher than the one at $P = 0.1\ \text{MPa}$. At 0.1 MPa, the system is either in transition or churn-turbulent flow while at 1.0 MPa, it is operating in bubbly flow regime. The reason for this discrepancy may be due to the change in flow regime or it can be an experimental error. However, this observation needs further examination and careful evaluation.

4. Summary

The improved CARPT technique (Rados, 2003) has been applied to study the solids motion and mixing characteristics in a pilot scale 0.162 m diameter high pressure stainless steel slurry bubble column. The effect of important operating parameters such as superficial gas velocity and pressure on solids axial velocity and shear stress in an air–water–glass beads ($150\ \mu\text{m}$) system has been studied. An increase in superficial gas velocity and operating pressure results in an increase in solids axial velocity. Because shear stress is proportional to the radial gradient of axial solids velocity, an increase in superficial gas velocity and operating pressure resulted in increased solids shear stress. Further studies to gain insight into the flow microstructure of slurry bubble column using CARPT and CT are in progress in our laboratory.

Acknowledgements

The authors are thankful for the financial support provided by DOE – UCR Grant (DE-FG-26-99FT40594) and indirectly by the High Pressure Slurry Bubble Reactor Consortium [ConocoPhillips (USA), EniTech (Italy), Sasol (South Africa), Statoil (Norway)], which made this work possible.

References

- CREL, 1993. Characterization of the liquid flow pattern and mixing in small diameter bubble columns via CARPT. Final technical report for the Statoil contract no. T-122.782, Washington University, St. Louis, MO.
- Deckwer, W.-D., Alper, E., 1980. Katalytische suspensions reaktoren. Chemical Engineering Technology 52, 219.
- Degaleesan, S., 1997. Fluid dynamic measurements and modeling of liquid mixing in bubble columns. D.Sc. Thesis, Washington University, St. Louis, MO.
- Devanathan, N., 1991. Investigation of liquid hydrodynamics in bubble columns via computer automated radioactive particle tracking (CARPT). D.Sc. Thesis, Washington University, St. Louis, MO.
- Dry, M.E., 1982. The SASOL route to fuels. CHEMTECH 12, 744.
- Fan, L.-S., 1989. Gas–Liquid–Solid Fluidization Engineering. Butterworths Series in Chemical Engineering, Boston, MA.
- Kemoun, A., Cheng Ong, B., Gupta, P., Al-Dahhan, M.H., Dudukovic, M.P., 2001. Gas holdup in bubble columns at elevated pressures via

- Computed Tomography. *International Journal of Multiphase Flow* 27 (5), 929.
- Krishna, R., de Swart, J.W.A., Ellenberger, J., Martina, G.B., Maretto, C., 1997. Gas holdup in slurry bubble columns: effect of column diameter and slurry concentration. *A.I.Ch.E. Journal* 33, 311.
- Kumar, S.B., Devanathan, N., Moslemian, D., Dudukovic, M.P., 1994. Effect of scale on liquid recirculation in bubble columns. *Chemical Engineering Science* 49, 5637.
- Rados, N., 2003. Slurry bubble column hydrodynamics. D.Sc. Thesis, Washington University, St. Louis, MO.
- Rados, N., Shaikh, A., Al-Dahhan, M.H., 2005. Phase distribution in a high pressure slurry bubble column via a single source computed tomography. *Canadian Journal of Chemical Engineering* 83, 104.
- Sannaes, B.H., 1997. Solids movement and concentration profiles in column slurry reactors. Dr. Ing. Thesis, Norwegian University of Science and Technology, Trondheim, Norway.
- Ueyama, K., Miyauchi, T., 1979. Properties of recirculating turbulent two phase flow in gas bubble columns. *A.I.Ch.E. Journal* 25, 258.
- Xue, J., 2004. Bubble velocity, size, and interfacial area measurements in bubble columns. D.Sc. Thesis, Washington University, St. Louis, MO.